

# Experimental Study of EGR Dilution and O<sub>2</sub> Enrichment Effects on Turbulent Non-premixed Swirling Flames

H. Zaidaoui<sup>1</sup>, T. Boushaki<sup>1,\*</sup>, JC. Sautet<sup>2</sup>, C. Chauveau<sup>1</sup>, B. Sarh<sup>1</sup>, I. Gökalp<sup>1</sup>

<sup>1</sup>ICARE CNRS, University of Orleans, Orléans, France

<sup>2</sup>Normandie University, CORIA, Saint Etienne du Rouvray, France

## 1 Introduction

Swirling flames are commonly utilized to stabilize diffusion flames in industrial applications, such as gas turbines, boilers and furnaces. The stabilization and the structure of the swirling flames depend on the swirl number, the burner geometry and the fuel injector [1-3]. This stabilization is due to the recirculation zones created by swirl flow which bring back hot gases to ignite the reactants, enhance the mixing of fuel and oxidizer and reduce flame temperature. Detailed descriptions of swirling flows could be found in literatures [4-6]. Worldwide, environmental regulations to limit pollutant emissions have been stringent. Consequently, the improvement of combustion equipment focuses mainly on reducing emissions, improving efficiency and lowering costs. Exhaust gas recirculation has great impact on fundamental combustion processes such as ignition and flame propagation as well as extinction. However, the influence of water vapor addition and exhaust gas recirculation on swirling flames stability and emissions have received less attention. The aim of the present work is to investigate the effects of exhaust gases recirculation, water vapour and CO<sub>2</sub>, with and without O<sub>2</sub> enrichment, on non-premixed turbulent flames stabilized by a swirl burner. The study focuses on pollutant emissions, flame stability through the determination of lift-off heights by analysing the emission of OH\* radicals and flow fields by LDV measurements. Different parameters of the burner are studied such as: the swirl number, the global equivalence ratio, and the fractions of O<sub>2</sub>, H<sub>2</sub>O and CO<sub>2</sub> in the mixture.

## 2 Experimental setup

The experiments have been carried out in a square cross-section chamber at atmospheric pressure. This combustion chamber of 1m high is comprised of six windows on each face allowing easy optical access to the flame. The burner placed at the bottom center of the chamber allows a vertical development of the

flame inside the combustion chamber. A detailed schematic representation of the coaxial swirl burner is shown in Figure 1.

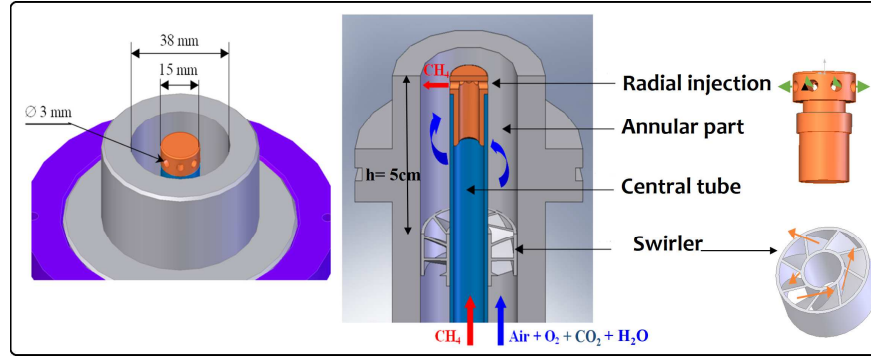


Figure 1. Coaxial swirl burner

The swirler contains 8 blades orientated according to the required swirl number and placed in the coaxial air-tube at 60 mm away from the burner. The central tube is used to supply methane from eight holes (3 mm diameter) with a radial injection. Note that the swirl number represents the ratio of the angular momentum flux  $G_\theta$  to the axial momentum flux  $G_z$  times a characteristic distance of the radial dimension  $R$ . It is defined as follows:

$$S_n = \frac{G_\theta}{R G_z} \quad (1)$$

The geometrical swirl number  $S_n$  for the present configuration can be expressed as:

$$S_n = \frac{1}{1-\psi} \cdot \left(\frac{1}{2}\right) \cdot \frac{1-(R_h/R)^4}{1-(R_h/R)^2} \tan \alpha_0 \quad (2)$$

where  $\alpha_0$  is the vane angle,  $\psi$  is the blockage factor and  $R$  and  $R_h$  are nozzle and vane pack hub radii respectively. Note that the swirl number could be calculated experimentally from 3D velocity measurements, as S-PIV.

The operating parameters are defined as follow: The oxygen content in the oxidizer ( $\Omega$ ) is the ratio of oxygen flow rate to the total flow rate (oxygen and nitrogen) expressed as:

$$\Omega = \frac{O_2}{O_2 + N_2} \quad (3)$$

The  $CO_2$ ,  $H_2O$  and EGR contents in the oxidizer is written as:

$$\% vol CO_2 = \frac{Q_{CO_2}}{Q_{air}}, \quad \% vol H_2O = \frac{Q_{H_2O}}{Q_{air}}, \quad \% vol EGR = \frac{Q_{H_2O} + Q_{CO_2}}{Q_{air}} \quad (4)$$

$\phi$  and  $S_n$  represent the global equivalence ratio and the swirl number respectively. In the present work, the oxidant flow rate remained fixed for all measurements, the global equivalence ratio varies from 0.8 to 1, the swirl number ranges from 0.8 to 1.4, the oxygen content in the oxidizer varies from 21% to 30% (in volume) in the oxidizer and the  $CO_2$  and  $H_2O$  contents range from 0% to 20% in volume.

#### *Chemiluminescence technique and gas analysis*

The chemiluminescence technique is used to study the spatial position of the flame reaction zones via the characterization of lift-off heights and flame lengths using OH\* radicals. The concentrations of NO<sub>x</sub>, CO, CO<sub>2</sub>, O<sub>2</sub> and SO<sub>2</sub> in the flue gases are measured using a HORIBA PG250 multi-gas analyser. These measuring techniques have been fully described in [7] for more details.

### *LDV system*

Laser Doppler Velocimetry system is used to describe the flow fields in reactive and non-reactive cases. Vertical and radial velocities,  $U(z, t)$  and  $V(x, t)$ , are measured by the new LDV system from TSI (PowerSight Solid State Laser, type TR-SS-2D). In this paper, only some first results of the axial component velocity are reported. There are two main modules for the powerSight system, the powerSight Laser Velocimeter and PowerSight Controller. PDM Photomultiplier module (PDM1000-2SS) and FSA signal processor (FSA 3500-2) are used with the module to make up the complete system. A couple of laser beams (532 and 561 nm, with 300 mW power, 2.1 mm of diameter) are used, each beam is split into two parallel beams which are focused to cross at the focal point of the transmitting lens of 750 mm. The distance between two laser beams is 50 mm and the size of measuring volume is 256  $\mu\text{m}$  and 245  $\mu\text{m}$  for the beam lasers 261 and 532 nm, respectively. The LDV results are displayed by FlowSizer 64 software. A 3D traverse system is set up to monitor the laser position relative to the burner center. The displacement is carried out in a horizontal way with a step of 1mm for different vertical positions ( $z$ ). The seeding particles of LDV measurements are Al<sub>2</sub>O<sub>3</sub> particles with about 0.5  $\mu\text{m}$  in diameter in reacting and non reacting flows.

## **3 Results and discussions**

### **3.1 Pollutant emissions**

Figure 2(a) shows the influence of CO<sub>2</sub> dilution on exhaust gas temperature, CO and NO<sub>x</sub> emissions in the case of 25% O<sub>2</sub> enrichment, at an equivalence ratio of 0.8 and a swirl number of 1.4. The results show that CO<sub>2</sub> addition reduces drastically the exhaust flame temperature. This might be due to the radiative and thermal effects related to the high specific heat of CO<sub>2</sub>, which reduces the overall heat release rate, and also the reduction of reactant concentrations in the mixture. This explains the NO<sub>x</sub> reduction from 45 ppm to almost 0 ppm in the case of 20% of CO<sub>2</sub> dilution, even for an oxygen enriched mixture. CO increases when adding CO<sub>2</sub> which is attributed to the chemical effect of CO<sub>2</sub>. However, the active participation of CO<sub>2</sub> in the chemical reactions through  $\text{CO} + \text{OH} = \text{CO}_2 + \text{H}$  makes the production and the oxidation of CO take a longer time. Consequently, the residence time is decreased and the heat release is slow [8].

Figure 2(b) shows the results obtained by varying water vapour amount in CH<sub>4</sub>/air mixture, with an equivalence ration of 0.8 and a swirl number of 1.4. The exhaust gas temperature reduces significantly with water vapour dilution, almost 100°K for 20% H<sub>2</sub>O, which reduces as well NO<sub>x</sub> emissions. We notice that CO concentration increases with H<sub>2</sub>O dilution. The lack of reactant amounts could be the main reason of this rise.

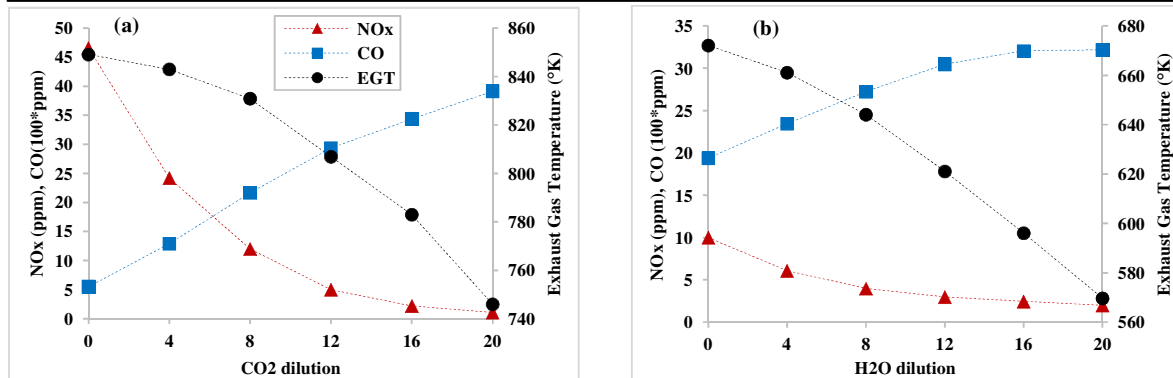


Figure 2. NOx, CO and EGT: (a): as function of CO<sub>2</sub>, at 25%O<sub>2</sub>,  $\phi=0.8$  and Sn=1.4. (b): a as a function of H<sub>2</sub>O dilution at 21%O<sub>2</sub>,  $\phi=0.8$  and Sn=1.4

### 3.2 OH\* Chemiluminescence results

OH\* chemiluminescence method is used to visualise flames in the case HO<sub>2</sub>, CO<sub>2</sub> and EGR dilutions with and without O<sub>2</sub> enrichments. In this paper, only the images of OH\* intensity in the case of H<sub>2</sub>O dilution are presented (Figure 3.). The OH\* chemiluminescence data allow to determine lift-off heights and lengths of flames following image processing of results. A Matlab image processing program (thresholding, binarization, filtering and contour detection) was developed to extract lift-off heights and flame lengths and the corresponding standard deviations. Figure 3 shows OH\* average images with H<sub>2</sub>O dilution in the case of Sn=0.8,  $\Phi=0.8$  and without O<sub>2</sub> enrichment (21%O<sub>2</sub>). It can be seen that the addition H<sub>2</sub>O increases the lift-off height of flame. The results display that the base of the flame becomes thinner and the flame is lengthened away from the burner. The OH\* intensity distributions illustrate the chemical effect of water vapour dilution.

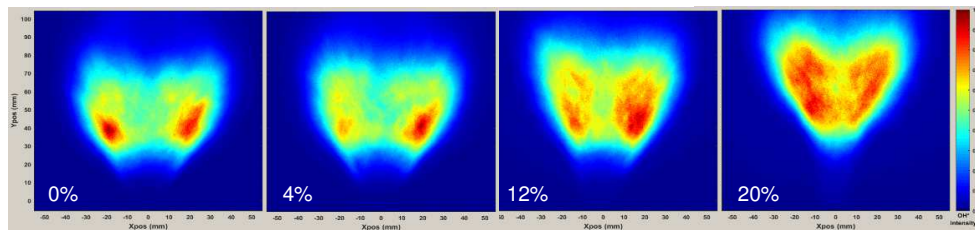


Figure 3. OH\* intensity distributions of H<sub>2</sub>O diluted CH<sub>4</sub>/air swirling flames at  $\phi=0.8$  and Sn=0.8

Flame lift-off heights with and without H<sub>2</sub>O or CO<sub>2</sub> dilution are shown in Figure 4(a). It can be observed that the dilution has significant effect on the flame lift-off heights. The case of CO<sub>2</sub> dilution is more significant than the H<sub>2</sub>O one. For both diluents, the lift-off height increases but the flame remains relatively stable until 20% of dilution. Figure 4(b) illustrates the flame lift-off height with O<sub>2</sub> rate in two cases: with EGR (10%CO<sub>2</sub>+10%H<sub>2</sub>O) and without EGR. The O<sub>2</sub> enrichment decreases the lift-off height and favors the flame stability. This stability is due to the main role of oxygen in enhancing the reaction rate which allows a fast gases burning near the burner. Figure 4(c) compares the effects of H<sub>2</sub>O addition on flame lift-off heights and their standard deviations (bars) for three swirl numbers (0.8, 1.1 and 1.4), 25% O<sub>2</sub> enriched CH<sub>4</sub>/air mixture and a global equivalence ratio of 0.8. These results reveal the strong effect of swirl intensity on lift-off height, since the difference is high for the three swirl numbers. It is noted that the addition of H<sub>2</sub>O increases slightly the flame position when the swirl intensity increases. This demonstrates that the effect of swirl is dominant in these cases.

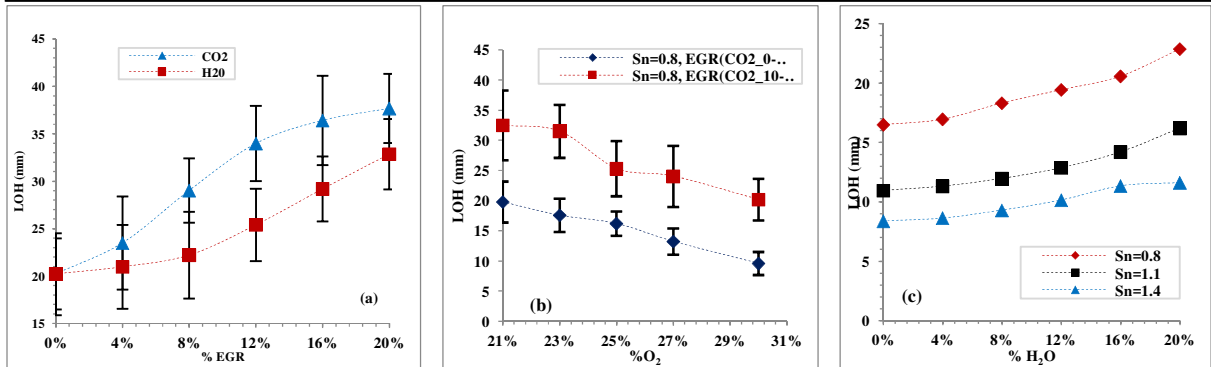


Figure 4. (a). Lift-off height with CO<sub>2</sub> and H<sub>2</sub>O dilutions for  $\phi=0.8$ , Sn=0.8 and 21%O<sub>2</sub>; (b): Lift-off height with O<sub>2</sub> enrichment with and without EGR; (c): lift-off heights with swirl/water vapor dilution for  $\phi=0.8$  and 25%O<sub>2</sub>.

### 3.3 LDV results

Figure 5 illustrates the results obtained by LDV measurements for a swirl number of 1.4 and  $\phi=0.8$  for the non reactive case. Figure 5(a) shows the radial profiles of axial velocity for 5 vertical along the flow. We can identify two hump shapes which specify the coaxial tube. The negative axial velocities in the center of the burner are related to the recirculation zone and the presence of the central tube. There is a slight difference between the right side and the left side because of the non-symmetry of the flow caused by the presence of swirler blades. Flow fluctuations are higher in the annular part and in the CRZ because the higher velocities of flow and layers mixing in these zones. The results of LDV measurements in reacting flow show that the combustion accelerates highly the flow as shown in Figure 6. It is also noted that the axial velocity decay is relatively slower. The dilution effect on flow velocity is reported in Figure 7 for the position  $z=30$  mm from the burner in the case of Sn=1.4 and  $\Phi=0.8$ . It is important to clarify that the flow rate of the oxidizer is kept constant with or without dilution. The Re number is varied between 4500 and 6000 because the variation of the mixture. In the case of CO<sub>2</sub>/HO<sub>2</sub> dilution, the maximum velocity is slightly higher and the flow is narrower.

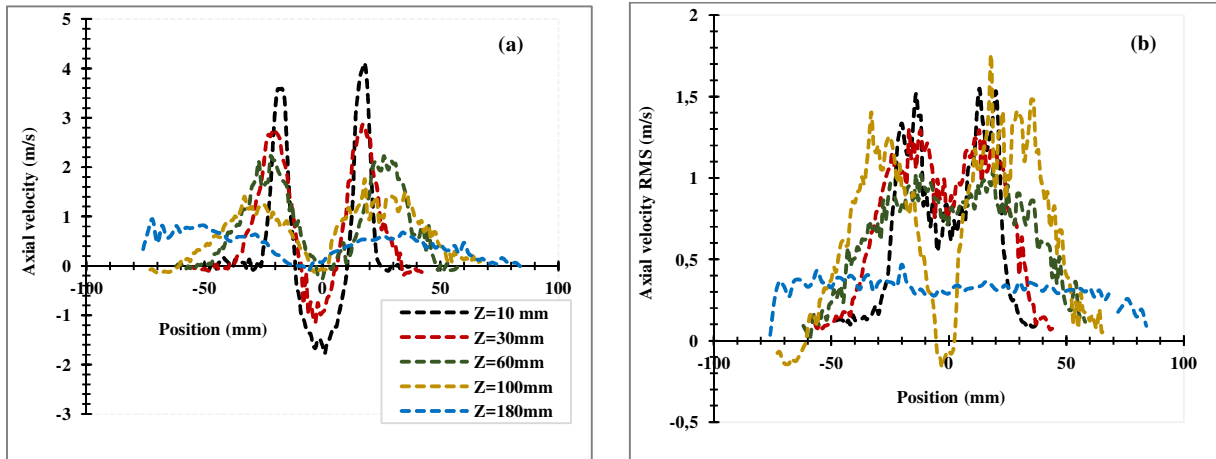


Figure 5. (a) Profiles of axial velocity of non reacting flow for 5 heights, Sn=1.4 and  $\phi=0.8$ . (b) Profiles of axial velocity RMS of non reacting flow.

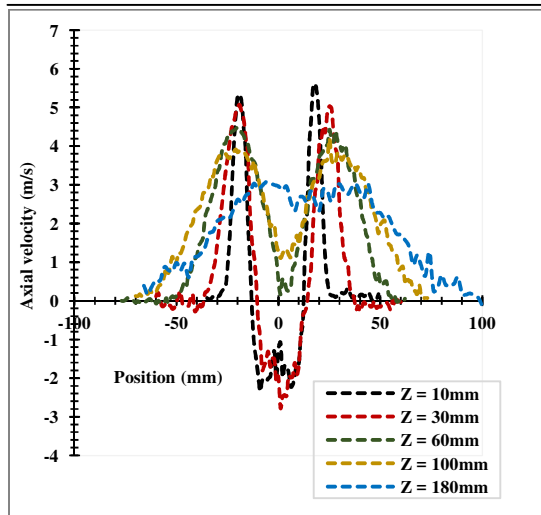


Figure 6. Profiles of axial velocity of reacting flow for 5 heights,  $Sn=1.4$  and  $\phi=0.8$ .

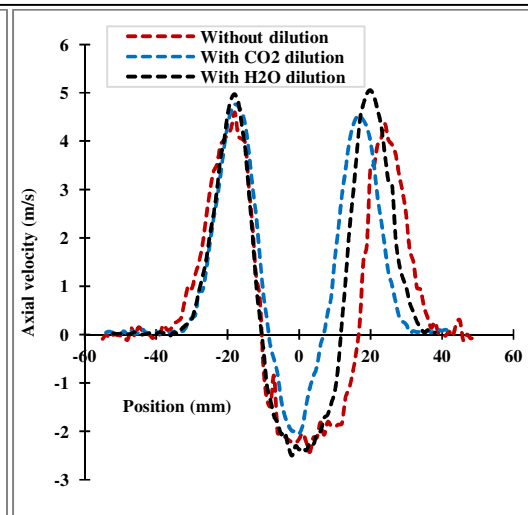


Figure 7. Comparison of profiles of axial velocity at  $z= 30$  mm with and without dilution.

#### 4 Conclusion

The present paper reports some experimental results of the EGR dilution ( $\text{CO}_2$ ,  $\text{H}_2\text{O}$ ,  $\text{CO}_2+\text{H}_2\text{O}$ ) effects on  $\text{CH}_4$ -air- $\text{O}_2$  flame characteristics. The burner used is swirled with a coaxial configuration and the flame is turbulent non-premixed. The fraction of diluents varies from 0 to 20%,  $\text{O}_2$  enrichment from 21 to 30% (in vol.) and the swirl number from 0.8 to 1.4. Results showed that the dilution has a significant influence on the flame behavior. With dilution the lift-off height increases but the flame remains stable. The  $\text{O}_2$  enrichment decreases the lift-off height and enhances the flame stability. The increase of dilution rate induces a decrease in  $\text{NO}_x$  emission and exhaust gas temperature and an increase in  $\text{CO}$  emissions. LDV measurements showed the axial velocity distribution of flow and its fluctuations in reactive and non reactive conditions. Note that the presence of the flame induces an increase in the axial velocity downstream of the flow due to the expansion of gases.

#### References

- [1] Syred N. A review of oscillation mechanisms and the role of the precessing vortex core (PVC) in swirl combustion systems. (2006). *Prog Energy Combust Sci.* 32:93–161.
- [2] Cheng R, Yegian D, Miyasato M, Samuelsen G, Benson C, Pellizzari R, et al. (2000). Scaling and development of low-swirl burners for low-emission furnaces and boilers. *Proc Comb Inst.* 28(1):1305–13.
- [3] Chtereov I, Sundararajan G, Seitzman J, Lieuwen T. (2015). Precession effects on the relationship between time-averaged and instantaneous swirl flow and flame characteristics. *ASME, GT2015-42768*.
- [4] Beér JM, Chigier NA. (1972). *Combustion Aerodynamics*. Applied Science Publishers Ltd;
- [5] Khalil AEE, Gupta AK. Swirling distributed combustion for clean energy conversion.
- [6] Archer S, Gupta A. (2013). Effect of Swirl on Flow Dynamics in Unconfined and Confined Gaseous Fuel Flames. In: *Aiaa Aerospace Sciences Meeting and Exhibit*.
- [7] Zaidaoui H, Boushaki T, Sautet JC, Chauveau C, Sarh B, Gokalp I. (2017). Effects of  $\text{CO}_2$  dilution and  $\text{O}_2$  enrichment on non-premixed turbulent  $\text{CH}_4$ -air flames in a swirl burner. *Combust Sci Technol* 190. 5:784-802.
- [8] Wang L, Liu Z, Chen S, Zheng C, Li J. (2013). Physical and chemical effects of  $\text{CO}_2$  and  $\text{H}_2\text{O}$  additives on counterflow diffusion flame burning methane, *Energy Fuels*. 27:7602–7611.